

## AN ANALYSIS OF THE SHOCK STRENGTH NEEDED TO ACHIEVE DEFIBRILLATION IN A SIMPLIFIED MATHEMATICAL MODEL OF CARDIAC TISSUE

ASLAK TVEITO<sup>1,2</sup>, GLENN LINES<sup>1,2</sup>, MARIE E. ROGNES<sup>1</sup>, AND MARY M.  
MALECKAR<sup>1</sup>

**Abstract.** The pumping function of the heart is driven by an electrical wave traversing the cardiac muscle in a well-organized manner. Perturbations to this wave are referred to as arrhythmias. Such arrhythmias can, under unfortunate circumstances, turn into fibrillation, which is often lethal. The only known therapy for fibrillation is a strong electrical shock. This process, referred to as defibrillation, is routinely used in clinical practice. Despite the importance of this procedure and the fact that it is used frequently, the reasons for defibrillation's effectiveness are not fully understood. For instance, theoretical estimates of the shock strength needed to defibrillate are much higher than what is actually used in practice. Several authors have pointed out that, in theoretical models, the strength of the shock can be decreased if the cardiac tissue is modeled as a heterogeneous substrate. In this paper, we address this issue using the bidomain model and the Courtemanche ionic model; we also consider a linear approximation of the Courtemanche model here. We present analytical considerations showing that for the linear model, the necessary shock strength needed to achieve defibrillation (defined in terms of a sufficiently strong change of the resting state) decreases as a function of an increasing perturbation of the intracellular conductivities. Qualitatively, these theoretical results compare well with computations based on the Courtemanche model. The analysis is based on an energy estimate of the difference between the linear solution of the bidomain system and the equilibrium solution. The estimate states that the difference between the linear solution and the equilibrium solution is bounded in terms of the shock strength. Since defibrillation can be defined in terms of a certain deviation from equilibrium, we use the energy estimate to derive a necessary condition for the shock strength.

**Key Words.** Defibrillation, Bidomain model, Energy estimate, Myocardial heterogeneities

### 1. Introduction

The beating of the human heart is a well-organized operation governed by an electrical wave which traverses the entire cardiac muscle to initiate contraction. This is a robust process, as it continues for about 80 years on average without maintenance, as well as versatile in the sense that it adapts smoothly to strongly varying external conditions. However, the heartbeat is not infallible. The regular electrical signal controlling the synchronous contraction of the heart may be disturbed. Such rhythm disturbances are known as arrhythmias and may result

---

Received by the editors January 25, 2011 and, in revised form, August 29, 2011.

in failure to adequately pump blood to the body. Ventricular fibrillation, an arrhythmia wherein the contraction of the heart muscle is completely asynchronous, is especially dangerous. If not treated within minutes, its ultimate consequence is sudden cardiac death [1].

Currently, the only effective means for prevention of sudden cardiac death is defibrillation of the heart by the timely application of a strong electric shock [2, 3, 4]. Significant advances have been made towards an improved understanding of the basic mechanisms by which a shock defibrillates the heart [5, 6, 7]. However, several key aspects of the interaction between an electric shock and the heart remain unclear. Hence, the mechanisms by which shocks terminate arrhythmias are far from fully understood. In recent years, mathematical modeling and simulation have had increasing importance in efforts to further understand the biophysical processes that underlie the generation of lethal arrhythmias and their termination via defibrillation [8, 9]. Simulations have offered not only increased understanding as to the mechanisms underlying defibrillation, but also valuable estimates of the amount of energy necessary to terminate fibrillation in a specific context [10, 11, 12].

Cardiac tissue, a functional syncytium, can be modeled mathematically via a continuum approximation, and fundamental ionic kinetics at the cell level by corresponding membrane models. However, when cardiac tissue is modeled via the bidomain approximation as a *homogeneous* substrate having uniform conductivities controlling current flow, simulations may result in an overestimation of the shock strength required for defibrillation [11]. Indeed, the assumption of homogeneity represents a simplification, as heterogeneities are realistic in terms of actual tissue structure. Such a simplification may yield results which are of questionable physiological relevance and limited clinical utility.

Microstructural myocardial heterogeneities have been previously represented in models through both random and localized alterations of conductivities and/or membrane kinetics [13, 14], as well as through realistic tissue discontinuities determined via high-resolution imaging [15, 16, 17]. The presence of larger-scale myocardial heterogeneities within computational bidomain models provides a substrate for bulk activation of the tissue following electric shocks, which may lower apparent estimates for defibrillation threshold. These larger-scale structures may include, for example, laminar clefts or vasculature, see [15, 18]. The inclusion of heterogeneities at multiple scales thus provides more realistic and lower estimates of the energy necessary to successfully defibrillate a particular substrate [19].

In this paper, we analyze the problem initially presented by Plank et al [20, 19]. These papers examine results obtained from simulations employing the bidomain model with cell membrane kinetics represented by the models of Courtemanche et al [21]. As outlined above, of particular interest is the result that the shock strength necessary to defibrillate decreases as tissue variability increases. Our aim is to contribute to a better understanding of this effect by providing theoretical estimates in addition to further numerical experiments.

The Courtemanche ionic model presents significant challenges to mathematical analysis. We have therefore introduced a linear approximation to the full model which we employ in its stead. In [22], it was demonstrated that this linear model provides fairly accurate solutions in the presence of strong shocks. In this paper, we present computational results examining the influence of random perturbations to the intracellular conductivities using both the full and the linear Courtemanche models. Furthermore, we provide analytical estimates for the linear model, showing that an increase in the variability of the intracellular conductivities leads to a

decrease in the necessary shock strength. This analytical result is thus in agreement with the earlier numerical observations.

For the purposes of mathematical analysis, we make certain assumptions regarding initial conditions. We assume that the tissue is at rest, and then analyze what shock strength is necessary to effect a sufficiently large change in the transmembrane potential as compared to a predefined threshold. This starting point is motivated by the assumption that the resting state is the most stable state the system can assume, and therefore the hardest state to significantly perturb. It follows that an estimate for the necessary energy to defibrillate; that is, initiate sufficient perturbation of the tissue, based on the resting state, should also apply for any other initial, less stable state.

**2. The mathematical models**

We consider a two-dimensional version of a problem presented by Plank et al [19, 20]. Let the domain be given by  $\Omega = (0, 4) \times (0, 2)$  cm<sup>2</sup> with boundary  $\partial\Omega$ ,  $t \in (0, T]$ , and consider the bidomain model

$$\begin{aligned} (1) \quad & v_t = \nabla \cdot (m_i \nabla v) + \nabla \cdot (m_i \nabla u) - I(v, s), \\ (2) \quad & I_e = \nabla \cdot (m_i \nabla v) + \nabla \cdot (m_{i+e} \nabla u), \\ (3) \quad & s_t = F(v, s), \end{aligned}$$

with the boundary conditions

$$(4) \quad (m_i \nabla v + m_i \nabla u) \cdot n = 0, \quad (m_i \nabla v + m_{i+e} \nabla u) \cdot n = 0 \quad \text{on } \partial\Omega,$$

and the initial condition

$$v(\cdot, \cdot, 0) = v_0.$$

In the system above  $v = v(x, y, t)$  is the transmembrane potential,  $u = u(x, y, t)$  is the extracellular potential,  $I_e = I_e(x, y)$  is a prescribed extracellular current (the defibrillation shock, scaled by  $(C_m \chi)^{-1}$ ),  $m_i = m_i(x, y)$  and  $m_e = m_e(x, y)$  are the intra- and extra-cellular conductivities and  $m_{i+e} = m_i + m_e$ . The conductivities are given by:

$$\begin{aligned} m_i &= \begin{pmatrix} \sigma_{ix} & 0 \\ 0 & \sigma_{iy} \end{pmatrix} = \frac{1}{C_m \chi} \begin{pmatrix} \hat{\sigma}_{ix} & 0 \\ 0 & \hat{\sigma}_{iy} \end{pmatrix}, \\ m_e &= \begin{pmatrix} \sigma_{ex} & 0 \\ 0 & \sigma_{ey} \end{pmatrix} = \frac{1}{C_m \chi} \begin{pmatrix} \hat{\sigma}_{ex} & 0 \\ 0 & \hat{\sigma}_{ey} \end{pmatrix}, \end{aligned}$$

where  $C_m$  is the membrane capacitance per unit area and  $\chi$  is the membrane surface-to-volume ratio. Furthermore,  $I$  denotes the total ionic current density, and  $F$  represents the electrochemical processes underpinning each action potential (the ionic model). From a physiological point of view, the natural boundary conditions are given by no-flow conditions on both the intra- and extracellular potentials. The form given in (4) above is derived from these conditions.

In the present paper, we will use the Courtemanche model [21] as modified by [19] (we employ  $B = 0$  in their model), and a linear model introduced in [22]. We will assume that (see [23])

$$\chi = 1400 \text{ cm}^{-1}, \quad C_m = 1.0 \mu\text{F}/\text{cm}^2,$$

and

$$\hat{\sigma}_{ex} = 6.25, \quad \hat{\sigma}_{ey} = 2.36, \quad \hat{\sigma}_{ix} = 1.46N(x, y), \quad \hat{\sigma}_{iy} = 0.19N(x, y),$$

all in mS/cm. Here  $N$  is given by

$$N = 1 + \varphi\eta.$$

where  $\eta$  is a random number uniformly distributed between  $-0.9$  and  $0.9$ , and  $\varphi$  is a control parameter ranging from  $0$  to  $1$ .

The full bidomain model coupled to complex and realistic models of cell electrophysiology is hard to approach via analytical tools. However, we have observed in [22] that a linear model of the total ionic current density provides good approximations in the context of analyzing defibrillation. Observe that this means that we approximate a fully nonlinear system of partial differential equations consisting of 22 equations to a linear system consisting of only two equations. This simplification enables much faster numerical solution and also offers the possibility of handling the system with analytical tools, such as an energy estimate. The purpose of the present paper is to use the linear model derived in [22] in order to provide theoretical insight into how the necessary shock strength to defibrillate depends on the variability of the intracellular conductivities. Our main approach is to derive an upper bound of the deviation from equilibrium via an energy estimate.

To this end, assume that the initial state  $v_0$  is a resting state. The linear model invokes the approximation

$$(5) \quad I(v, s) = \alpha(v - v_0)$$

where  $\alpha$  will be specified below. Introducing  $v := v - v_0$ , we then obtain the system

$$(6) \quad v_t = \nabla \cdot (m_i \nabla v) + \nabla \cdot (m_i \nabla u) - \alpha v,$$

$$(7) \quad I_e = \nabla \cdot (m_i \nabla v) + \nabla \cdot (m_{i+e} \nabla u).$$

We equip the system defined by (6) and (7) with the boundary conditions given by (4) and the initial condition  $v(0, \cdot) = 0$ .

In order to have a unique solution of the extracellular potential  $u$ , we impose the additional requirement

$$(8) \quad \int_{\Omega} u = 0,$$

and the corresponding compatibility condition for the extracellular current  $I_e$ :

$$\int_{\Omega} I_e = 0.$$

Moreover, it follows from (4), (6), and the fact that  $\int v(0) = 0$  that

$$(9) \quad \int_{\Omega} v = 0.$$

Note that this observation does not hold in the nonlinear case.

We introduce the standard  $L^2(\Omega; \mathbb{R}^n)$  inner product and norm:

$$\langle u, v \rangle = \int_{\Omega} u \cdot v \, dx, \quad \|u\|^2 = \langle u, u \rangle.$$

A natural variational form of the system defined by (6) and (7) reads: find  $v(t) \in V$  and  $u(t) \in V$  such that

$$(10) \quad \langle v_t, w \rangle + \langle m_i \nabla v, \nabla w \rangle + \langle m_i \nabla u, \nabla w \rangle + \langle \alpha v, w \rangle = 0 \quad \forall w \in V,$$

$$(11) \quad \langle m_i \nabla v, \nabla q \rangle + \langle m_{i+e} \nabla u, \nabla q \rangle = -\langle I_e, q \rangle \quad \forall q \in V.$$

In Figure 1, we have compared the solution at time  $t = 5\text{ms}$  using the Courtemanche model and the linear model with  $\alpha = 0.1$ . In corresponding computations, we have used a uniform mesh with  $\Delta x = \Delta y = 0.2\text{mm}$  and  $\Delta t = 0.05\text{ms}$ . We

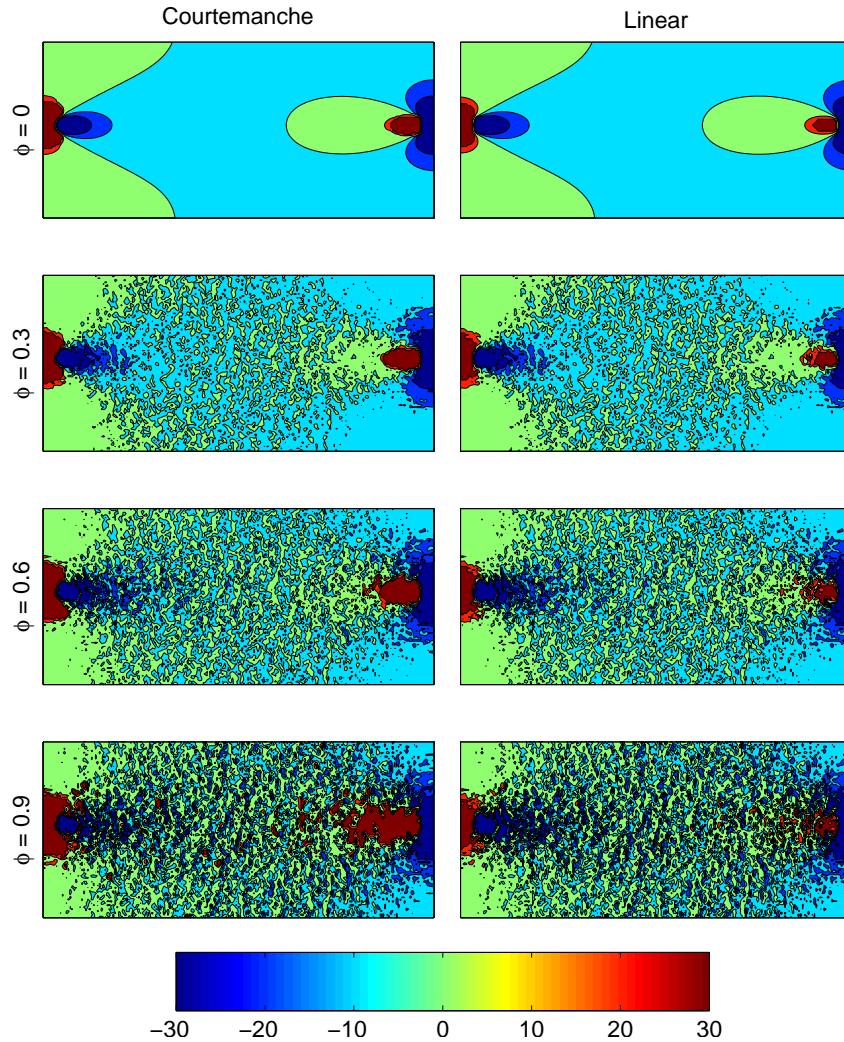


FIGURE 1. The transmembrane potential at  $t = 5\text{ms}$  of bidomain computations using a Courtemanche cell model (left) and linear model (right). The variability of the medium is increased for  $\varphi = 0$  (upper row) to  $\varphi = 0.9$  (lower row). We observe that, in all cases, the linear model provides reasonable approximations.

have used a common random field  $\eta$ , and then varied the strength of the variations in conductivity by choosing  $\varphi = 0, 0.3, 0.6, 0.9$ . Furthermore, we have applied an electric shock (scaled by  $1/C_m\chi$ ) given by:

$$I_e = \begin{cases} 1400\text{mV/ms} & (x, y) \in [0, 0.95] \times [0.1, 1.05], \\ -1400\text{mV/ms} & (x, y) \in [3.9, 0.95] \times [4, 1.05], \\ 0 & \text{for all other } (x, y). \end{cases}$$

We observe that for all choices of  $\varphi$ , the results of the linear model and the Courtemanche model are quite similar. Further comparison of these models is provided in [22]. The numerical method used to solve the problem is presented in Section 4.

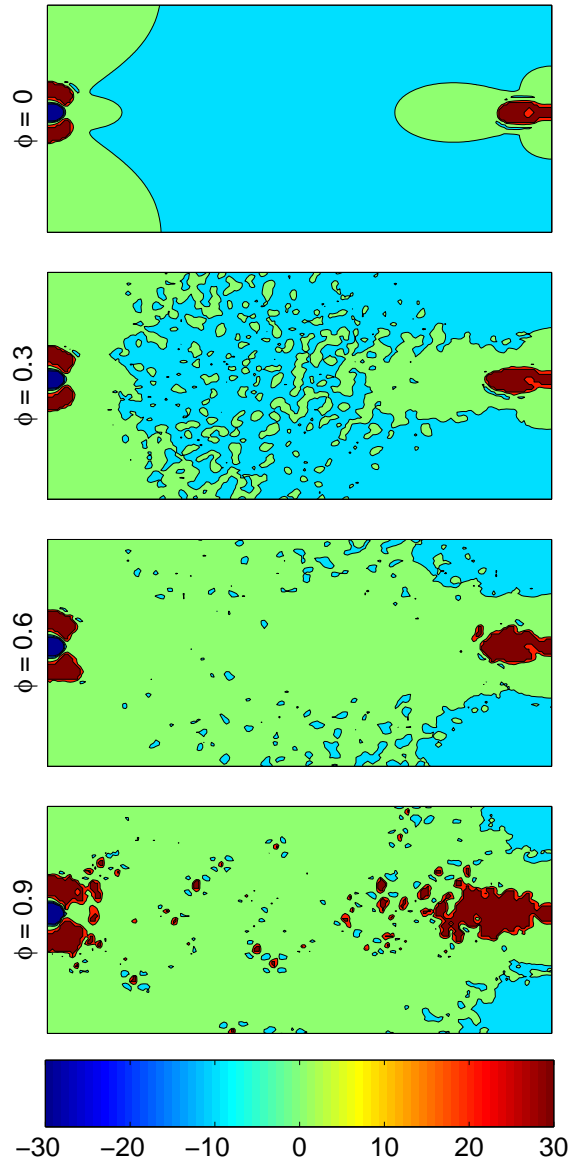


FIGURE 2. The difference between the solution provided by the Courtemanche cell and linear model for the parameters analyzed in Figure 1 above. The error is largest around around the poles, and rather small in the interior of the domain.

### 3. A theoretical requirement on the prescribed defibrillation shock

The purpose of this section is to derive a necessary condition for achieving defibrillation when considering the linear model presented above.

**3.1. Definition of defibrillation.** We *assume* that defibrillation is achieved at time  $t = t^*$  provided that the norm of  $v$  exceeds a certain threshold  $v^*$ ; i.e. provided that

$$\|v(t^*)\| \geq v^*.$$

The aim of this section is to provide an upper bound of the norm of  $v$  solving (10) and (11), in terms of the strength of the defibrillation shock  $I_e$ . The bound will take the form

$$\|v(t)\| \leq c(t) \|I_e\|$$

where the function  $c(t)$  is to be estimated. Combining the bound and the threshold, we can conclude that a necessary condition for defibrillation is given by

$$(12) \quad \|I_e\| \geq \frac{v^*}{c(t^*)}.$$

Moreover, we want to assess the consequences of this estimate in terms of the current needed to bring about a successful defibrillation. In particular, we want to analyze how the necessary strength of the defibrillation current depends on the variability  $\varphi$  of the medium.

**3.2. An energy estimate.** We begin by making some observations. From the definitions of  $m_i$  and  $m_e$ , there are positive constants  $a_i^-, a_i^+, a_e^-, a_e^+$  such that

$$(13) \quad a_i^- \langle \nabla w, \nabla w \rangle \leq \langle m_i \nabla w, \nabla w \rangle \leq a_i^+ \langle \nabla w, \nabla w \rangle$$

$$(14) \quad a_e^- \langle \nabla w, \nabla w \rangle \leq \langle m_e \nabla w, \nabla w \rangle \leq a_e^+ \langle \nabla w, \nabla w \rangle$$

for all  $w \in V = H^1(\Omega; \mathbb{R}^2)$ . In particular, we have

$$a_e^- \leq \sigma_{ex}, \sigma_{ey} \leq a_e^+, \quad a_i^- \leq \sigma_{ix}, \sigma_{iy} \leq a_i^+$$

with

$$a_e^- = 2.36/1400, \quad a_e^+ = 6.25/1400,$$

$$a_i^- = a_i^-(\varphi) = \frac{0.19}{1400}(1 - \varphi), \quad a_i^+ = a_i^+(\varphi) = \frac{1.46}{1400}(1 + \varphi).$$

It follows in particular that for all  $w \in V$

$$(15) \quad \langle m_i \nabla w, \nabla w \rangle \leq \beta \langle m_{i+e} \nabla w, \nabla w \rangle \quad \text{where } \beta = \frac{a_i^+}{a_e^- + a_i^+} < 1.$$

Also observe that because of (8) and (9), Poincaré’s inequality states that there exists a  $C > 0$  such that for  $u$  and  $v$  solving (10) and (11),

$$(16) \quad \|w\| \leq C \|\nabla w\| \quad \text{for } w \in \{u, v\}.$$

The following lemma gives an upper bound for  $v$  and hence an estimate for the function  $c$  in (12).

**Lemma 1.** *Let  $v(t)$  and  $u(t)$  solve (10) and (11) with  $v(0) = 0$  and prescribed  $\alpha$ . Then*

$$\|v(t)\| \leq c(t) \|I_e\|$$

where

$$(17) \quad c(t)^2 = c_1 c_0^{-1} (1 - e^{-c_0 t}), \quad c_0 = 2(\alpha + \gamma a_i^- C^{-2}), \quad c_1 = \frac{C^2}{2\gamma a_{i+e}^-}.$$

Here,  $C$  is given by (16),  $a_{i+e}^- = a_i^- + a_e^-$ ,  $a_i^-$  and  $a_e^-$  are given by (13),  $\gamma = 1 - \beta^{1/2}$ , and  $\beta$  is defined by (15).

*Proof.* Let  $w = v$  in (10) and  $q = u$  in (11) and add the equations to obtain

$$(18) \quad \begin{aligned} \langle v_t, v \rangle + \langle m_i \nabla v, \nabla v \rangle + \langle \alpha v, v \rangle + \langle m_{i+e} \nabla u, \nabla u \rangle \\ = -\langle I_e, u \rangle - 2\langle m_i \nabla u, \nabla v \rangle. \end{aligned}$$

Recall Cauchy's inequality with  $\epsilon$ , stating that for any inner product  $a$

$$(19) \quad |a(u, v)| \leq \epsilon a(u, u) + \frac{1}{4\epsilon} a(v, v) \quad \forall u, v, \epsilon > 0.$$

Using (19) for (the absolute value of) the right-hand sides of (18), we have

$$(20) \quad \begin{aligned} \langle v_t, v \rangle + \langle m_i \nabla v, \nabla v \rangle + \langle \alpha v, v \rangle + \langle m_{i+e} \nabla u, \nabla u \rangle \\ \leq \epsilon \langle u, u \rangle + \frac{1}{4\epsilon} \langle I_e, I_e \rangle + \delta \langle m_i \nabla v, \nabla v \rangle + \frac{1}{\delta} \langle m_i \nabla u, \nabla u \rangle \end{aligned}$$

for any  $\epsilon, \delta > 0$ . Applying (15) to the right-most term of (20) and moving the terms involving  $\delta$  across the inequality, we obtain

$$\langle v_t, v \rangle + (1 - \delta) \langle m_i \nabla v, \nabla v \rangle + \langle \alpha v, v \rangle + (1 - \frac{\beta}{\delta}) \langle m_{i+e} \nabla u, \nabla u \rangle \leq \epsilon \langle u, u \rangle + \frac{1}{4\epsilon} \langle I_e, I_e \rangle.$$

We can now choose  $\delta$  and  $\epsilon$ . First, let  $\delta = \beta^{1/2}$  and define  $\gamma = 1 - \beta^{1/2} > 0$ . This choice yields

$$\langle v_t, v \rangle + \gamma \langle m_i \nabla v, \nabla v \rangle + \langle \alpha v, v \rangle + \gamma \langle m_{i+e} \nabla u, \nabla u \rangle \leq \epsilon \langle u, u \rangle + \frac{1}{4\epsilon} \langle I_e, I_e \rangle.$$

Second, using (16) for  $u$ , (13), and (14), we find that

$$\langle u, u \rangle \leq C^2 \langle \nabla u, \nabla u \rangle \leq \frac{C^2}{a_{i+e}^-} \langle m_{i+e} \nabla u, \nabla u \rangle,$$

and thus

$$\langle v_t, v \rangle + \gamma \langle m_i \nabla v, \nabla v \rangle + \langle \alpha v, v \rangle + (\gamma - \epsilon \frac{C^2}{a_{i+e}^-}) \langle m_{i+e} \nabla u, \nabla u \rangle \leq \frac{1}{4\epsilon} \langle I_e, I_e \rangle.$$

Taking  $\epsilon = \gamma a_{i+e}^- C^{-2}$  and using (16) for  $v$ , we find that

$$\langle v_t, v \rangle + (\alpha + \gamma a_i^- C^{-2}) \langle v, v \rangle \leq \frac{C^2}{4\gamma a_{i+e}^-} \langle I_e, I_e \rangle.$$

Since  $2\langle v_t, v \rangle = \frac{d}{dt} \|v\|^2$ , Grönwall gives the stated result. □

**Remark 2.** *The same argument holds for the case of homogeneous Dirichlet boundary conditions.*

**Remark 3.** *The same argument holds for spatially discrete solutions  $v_h(t)$  and  $u_h(t)$  solving (10) and (11) for all  $w \in V_h$  and  $q \in V_h$  when  $V_h \subseteq V$ .*

**3.3. Physiological interpretation of the theoretical estimate.** We have proved that

$$(21) \quad \|v(t)\| \leq c(t, \varphi) \|I_e\|$$

where  $c(t, \varphi)$  is given by (17). By assuming that defibrillation is achieved at time  $t = t^*$  if  $\|v(t)\| \geq v^*$ , we see, as above, that we need the strength to satisfy  $\|I_e\| \geq v^*/c(t^*, \varphi)$ . Let us define this to be the minimum shock strength at time  $t = t^*$ ; i.e.

$$(22) \quad g(\varphi) = \frac{v^*}{c(t^*, \varphi)}.$$



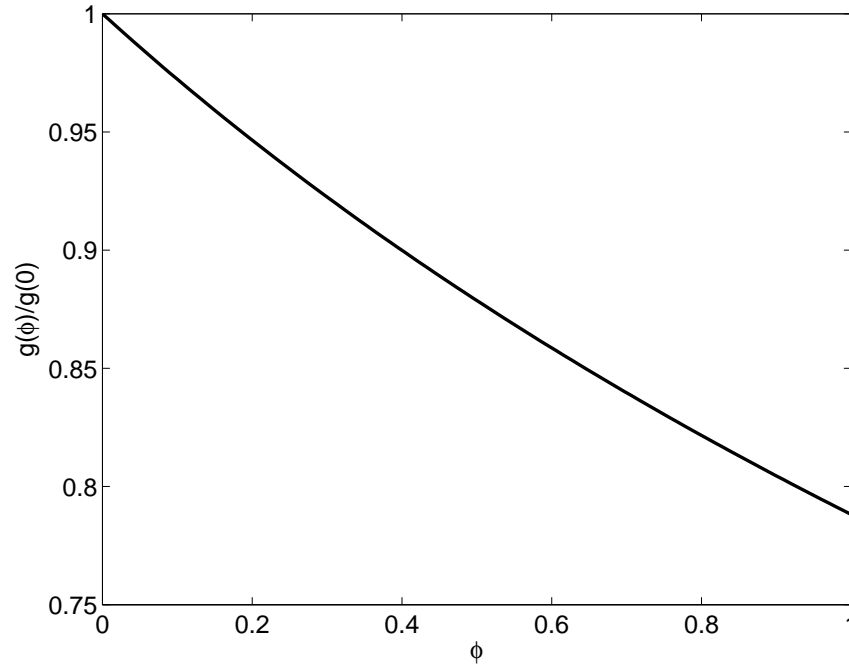


FIGURE 3. Plot of the analytically estimated minimum shock strength  $g(\varphi)$ , cf. (22), scaled by the estimated minimum shock strength at zero variability  $g(0)$ , versus the variability  $\varphi$ . We observe that the minimal shock strength decreases as the intracellular variability increases.

In Figure 3 we plot the function  $g(\varphi)/g(0)$  as a function of the variability  $\varphi$  in the case of  $\alpha = 0.05$  and  $t^* = 5$ . Here, we have used the Poincaré constant  $C = \frac{4}{\pi}$ ; it is explained in e.g. [24] how this constant can be computed for rectangular domains. We observe that the minimal shock strength based on this theoretical estimate is a decreasing function of the variability  $\varphi$  of the intracellular conductivity. This result is in accordance with the results of Plank et al [19, 20], which suggested that small-scale conductivity fluctuation is a very important factor in defibrillation, as a higher variation significantly lowered the shock strength required to defibrillate in their numerical experiments.

#### 4. Numerical experiments

**4.1. Numerical method.** Many numerical methods have been developed for solving the bidomain system (1, 2, 3); see e.g. [25, 26]. In the present paper, we are primarily interested in the qualitative properties of the solution of the system for the geometry described above. Since the geometry is simple, we use a finite difference approach to solve the system. Given a uniform mesh with spacing  $\Delta x$  and  $\Delta y$  in the  $x$ - and  $y$ - directions, respectively, we use standard finite difference approximations of the form

$$(23) \quad \frac{\partial}{\partial x} \left( m(x, y) \frac{\partial v(x_j, y_k)}{\partial x} \right) \approx \frac{m_{j+1/2, k}(v_{j+1, k} - v_{j, k}) - m_{j-1/2, k}(v_{j, k} - v_{j-1, k})}{(\Delta x)^2}$$

where  $v_{j,k}$  denotes an approximation of  $v(x_j, y_k)$  and where  $(x_j, y_k)$  denote nodes in the computational mesh. Similarly, we have  $m_{j+1/2,k} = m(x_{j+1/2}, y_k)$ . Using these approximations for the spatial derivatives in the bidomain system, we obtain the following system of differential-algebraic equations

$$(24) \quad v' = A_i v + A_i u - I(v, s),$$

$$(25) \quad I_e = A_i v + A_{i+e} u,$$

$$(26) \quad s' = F(v, s).$$

Here  $u, v$  and  $s$  carry the nodal approximations of the associated continuous variables,  $I_e$  carries nodal values of the electrical shock and the matrices  $A_i, A_e$  represent terms involving spatial derivatives in the system, with  $A_{i+e} = A_i + A_e$ . It follows from the system (1, 2, 3) that if  $(v, u, s)$  is a solution of the the system, then also  $(v, u + \alpha, s)$  is a solution for any constant  $\alpha$ . Hence the matrix  $A_{i+e}$  is singular. Using an iterative method as described in e.g. [27], the singularity is not a problem, but here we want to eliminate the extracellular potential  $u$  from the system, and thus we need  $A_{i+e}$  to be non-singular. Theoretically, this can be achieved by imposing the condition (8), but in computations we achieve this by adding a small regularization term of the form  $-\varepsilon u$  to the right-hand side of (2) and introduce the matrix

$$(27) \quad A_{i+e,\varepsilon} = A_{i+e} - \varepsilon J$$

where  $J$  is the identity matrix and  $\varepsilon > 0$  is small number. In the computations we have used  $\varepsilon = 10^{-6}$ . Numerical experiments show that the results are robust with respect to small changes of this parameter.

We now have the system (24, 25, 26) where  $A_{i+e}$  is replaced by  $A_{i+e,\varepsilon}$ . From (25), we get

$$(28) \quad u = A_{i+e,\varepsilon}^{-1} (I_e - A_i v)$$

and thus we have the system,

$$(29) \quad v' = (J - A_i A_{i+e,\varepsilon}^{-1}) A_i v + A_i A_{i+e,\varepsilon}^{-1} I_e - I(v, s),$$

$$(30) \quad s' = F(v, s).$$

This is a system of ordinary differential equations and we solve it using the generalized Rush-Larsen scheme presented in [28].

**4.2. Computations.** The theoretical estimates presented in the previous indicate that the necessary shock strength needed to achieve defibrillation decreases as the variability of the intracellular conductivities increases. This effect has also been observed in computations by several authors (see e.g. Plank et al [20, 19]). Here, we address this issue computationally using the bidomain model combined with the modified Courtemanche model and the linear model described above.

For a sample set of values for  $\varphi$ , we performed a series of simulations with varying shock strengths  $I_e$ . For each case, the norm of the computed  $v$  was recorded and compared to the critical threshold  $v^*$ . All computations used the finite difference method as described above, and the mesh parameters were the same as those used for Figure 1. Several other mesh parameters have been used with similar qualitative results. With these data, we used a spline curve fit to estimate the critical shock strength  $I_{\text{critical}} = I_{\text{critical}}(\varphi)$  at which the norm of the solution exceeds the threshold.

The results for both the Courtemanche and the linear model are presented in Figure 4. The graphs show the scaled critical shock strength  $I_{\text{crucial}}(\varphi)/I_{\text{critical}}(0)$

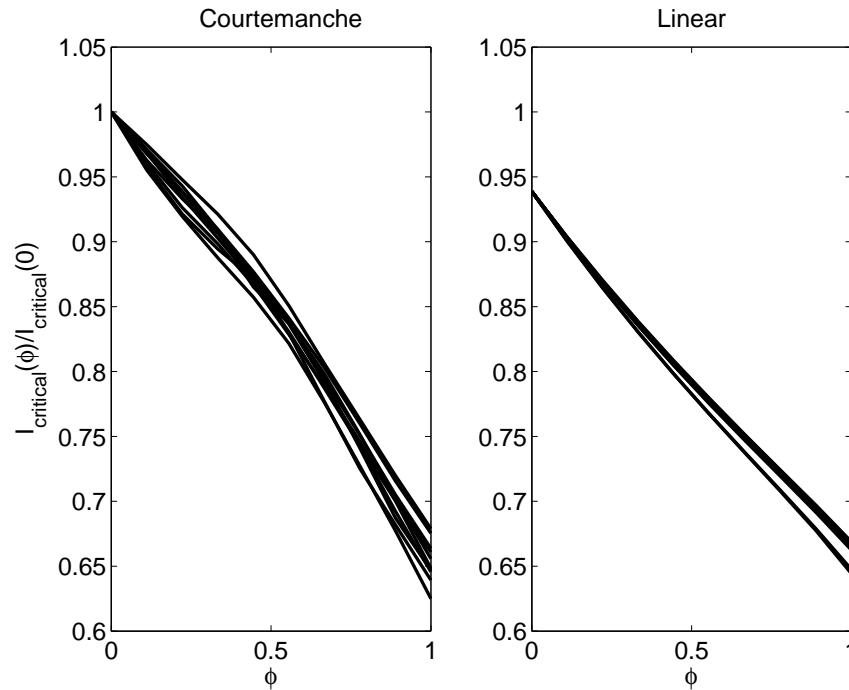


FIGURE 4. Plot of the numerically estimated critical shock strengths  $I_{\text{critical}}(\varphi)$  for the modified Courtemanche (left) and the linear (right) model, scaled by the critical shock strength at zero variability for the Courtemanche model  $I_{\text{critical}}(0)$ , versus the variability of the intracellular conductivities  $\varphi$ . Each line in each plot corresponds to one realization of the random field  $\eta = \eta(x, y)$ . The shock strength necessary to defibrillate decreases as the variability increases.

versus the variability  $\varphi$ . A common scale is used to enable direct comparison of the results for the two models: the scale  $I_{\text{critical}}(0)$  is, in both plots, the critical shock strength estimated for the Courtemanche model with zero variability, and is approximately 1280 mV/ms. Moreover, each line in the plots in Figure 4 corresponds to one realization of the random field  $\eta = \eta(x, y)$ . We observe that, for both ionic models, the necessary shock strength decreases as the control parameter  $\varphi$  increases. In addition, we note that the linear model in Figure 4 (right panel) provides reasonable approximations of the shock strength necessary for defibrillation in the Courtemanche model.

Comparing the analytical and the numerical results for the linear model, Figure 3 and Figure 4 (right panel), we observe that the numerical estimate and the analytical estimate both show the same trend: the necessary shock strength decreases as the variability increases. Moreover, their rate of decay is comparable. We remark however that the numerical estimates are approximately three orders of magnitude higher than the analytical estimates. A certain underestimation by the analytical estimate is expected though, as the analysis provides a lower bound for the necessary shock strength.

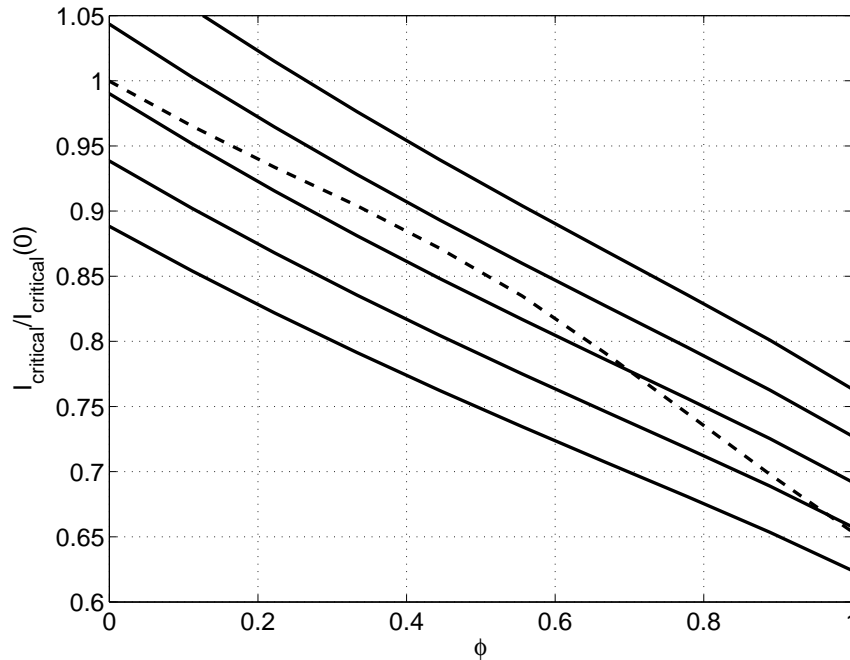


FIGURE 5. Sensitivity analysis for  $\alpha$ . Plots of the numerically estimated scaled critical shock strengths, cf. Figure 4, versus variability  $\varphi$  for varying  $\alpha$ . The dotted line represent the behavior of the Courtemanche model averaged over the realizations of the random fields  $\eta$  from Figure 4. The solid lines show the behavior for the linear model for various choices of  $\alpha$ . From bottom to top:  $\alpha = 0.075, 0.1, 0.125, 0.15, 0.175$ .

In Figure 5, we illustrate the effect of changes in the linearization parameter  $\alpha$ , see (5). According to results as presented in Figure 5,  $\alpha = 0.1$  provides a reasonable approximation to the Courtemanche model and this value is used in the computations using the linear model presented in Figure 4.

In the computations presented here, we have used  $t^* = 5\text{ms}$ , which is consistent with similar experiments presented in e.g. [19]. Numerical experiments shown here reveal that by increasing  $t^*$ , we can reduce the needed shock strength to defibrillate, as expected based on the theoretical estimate also presented above.

## 5. Conclusion

It has been observed previously that the shock strength needed to achieve defibrillation decreases when the variability of the intracellular conductivities increases. In this paper, we have analyzed a linear model and derived a necessary condition for defibrillation for that model. An energy estimate is used to derive the condition given in terms of an upper bound for the deviation between the linear solution of the bidomain model and the equilibrium solution. The theoretical estimate states that the necessary shock strength decreases as the variability of the medium increases. This effect is also confirmed by computations presented here.

The linear model used in the present paper was adopted from [22]. Numerical experiments show that the approximations provided by the model are accurate

and the theoretical considerations presented here show that the system is tractable with mathematical tools. Additionally, the linear system is extremely simple when compared to the original ionic model. Such an approximation of membrane kinetics is easy to handle computationally, and trivial to integrate into tissue- and organ-level finite element models of cardiac electrophysiology. Such a linear model may thus be desirable for application in future, and perhaps personalized, studies of defibrillation employing high-resolution, anatomically accurate models of the heart.

## 6. Acknowledgement

The first author would like to express his gratitude for many years of support and supervision from professor Magne Espedal both in scientific and political issues.

## References

- [1] Heart Rhythm Foundation. Sudden cardiac arrest key facts, January 2010. <http://www.heartrhythmfoundation.org/facts/scd.asp>.
- [2] Craig Pratt. Clinical implications of the survival with oral d-sotalol (sword) trial: An investigation of patients with left ventricular dysfunction after myocardial infarction. *Cardiac Electrophysiology Review*, 2:28–29, 1998.
- [3] American Heart Association. Sudden death from cardiac arrest: statistics, 2004. <http://www.americanheart.org>.
- [4] Gust H. Bardy, Kerry L. Lee, Daniel B. Mark, Jeanne E. Poole, Douglas L. Packer, Robin Boineau, Michael Domanski, Charles Troutman, Jill Anderson, George Johnson, Steven E. McNulty, Nancy Clapp-Channing, Linda D. Davidson-Ray, Elizabeth S. Fraulo, Daniel P. Fishbein, Richard M. Luceri, and John H. Ip. Amiodarone or an implantable cardioverter-defibrillator for congestive heart failure. *New England Journal of Medicine*, 352(3):225–237, 01 2005.
- [5] T. Ashihara, J. Constantino, and N. A. Trayanova. Tunnel propagation of postshock activations as a hypothesis for fibrillation induction and isoelectric window. *Circ Res*, 102(6):737–45, 2008.
- [6] N. Trayanova and Ed. J. Jalife G. Plank. *Modeling cardiac defibrillation*, In: *Cardiac Electrophysiology: From Cell to Bedside*, page 361372. WB Saunders, Philadelphia, 2009.
- [7] D. J. Dossdall, V. G. Fast, and R. E. Ideker. Mechanisms of defibrillation. *Annu Rev Biomed Eng*, 12:233–58, 2010.
- [8] G. I. Fishman, S. S. Chugh, J. P. Dimarco, C. M. Albert, M. E. Anderson, R. O. Bonow, A. E. Buxton, P. S. Chen, M. Estes, X. Jouven, R. Kwong, D. A. Lathrop, A. M. Mascette, J. M. Nerbonne, B. O’Rourke, R. L. Page, D. M. Roden, D. S. Rosenbaum, N. Sotoodehnia, N. A. Trayanova, and Z. J. Zheng. Sudden cardiac death prediction and prevention: report from a national heart, lung, and blood institute and heart rhythm society workshop. *Circulation*, 122(22):2335–48, 2010.
- [9] N. A. Trayanova. Whole-heart modeling: applications to cardiac electrophysiology and electromechanics. *Circ Res*, 108(1):113–28, 2011.
- [10] J. L. Jones and O. H. Tovar. Threshold reduction with biphasic defibrillator waveforms. role of charge balance. *J Electrocardiol*, 28 Suppl:25–30, 1995.
- [11] J. P. Keener. Direct activation and defibrillation of cardiac tissue. *J Theor Biol*, 178(3):313–24, 1996.
- [12] A. L. de Jongh, E. G. Entcheva, J. A. Replogle, 3rd Booker, R. S., B. H. Kenknight, and F. J. Claydon. Defibrillation efficacy of different electrode placements in a human thorax model. *Pacing Clin Electrophysiol*, 22(1 Pt 2):152–7, 1999.
- [13] K. H. Ten Tusscher and A. V. Panfilov. Influence of diffuse fibrosis on wave propagation in human ventricular tissue. *Europace*, 9 Suppl 6:vi38–45, 2007.
- [14] Brock M. Tice, Blanca Rodriguez, James Eason, and Natalia Trayanova. Mechanistic investigation into the arrhythmogenic role of transmural heterogeneities in regional ischaemia phase 1a. *Europace*, 9(suppl 6):vi46–vi58, 2007.
- [15] D A Hooks, K A Tomlinson, S G Marsden, I LeGrice, B H Smaill, A J Pullan, and P J Hunter. Cardiac microstructure; implications for electrical propagation and defibrillation in the heart. *Circulation Research*, 91:331–338, 2002.

- [16] D. A. Hooks, M. L. Trew, B. J. Caldwell, G. B. Sands, I. J. Legrice, and B. H. Smaill. Laminar arrangement of ventricular myocytes influences electrical behavior of the heart. *Circ Res*, 2007.
- [17] Gernot Plank, Rebecca A.B. Burton, Patrick Hales, Martin Bishop, Tahir Mansoori, Miguel O. Bernabeu, Alan Garny, Anton J. Prassl, Christian Bollensdorff, Fleur Mason, Fahd Mahmood, Blanca Rodriguez, Vicente Grau, Jrgen E. Schneider, David Gavaghan, and Peter Kohl. Generation of histo-anatomically representative models of the individual heart: tools and application. *Philosophical Transactions of the Royal Society A: Mathematical, Physical and Engineering Sciences*, 367(1896):2257–2292, 2009.
- [18] M. J. Bishop, P. M. Boyle, G. Plank, D. G. Welsh, and E. J. Vigmond. Modeling the role of the coronary vasculature during external field stimulation. *IEEE Trans Biomed Eng*, 57(10):2335–45, 2010. Bishop, Martin J Boyle, Patrick M Plank, Gernot Welsh, Donald G Vigmond, Edward J 085605/Wellcome Trust/United Kingdom Wellcome Trust/United Kingdom Research Support, Non-U.S. Gov't United States IEEE transactions on bio-medical engineering IEEE Trans Biomed Eng. 2010 Oct;57(10):2335-45. Epub 2010 Jun 10.
- [19] G. Plank, L. J. Leon, S. Kimber, and E.J. Vigmond. Defibrillation depends on conductivity fluctuations and the degree of disorganization in reentry patterns. *J Electrophysiol*, 16:205–216, 2005.
- [20] G. Plank, E. J. Vigmond, and L. J. Leon. Shock energy for successful defibrillation of atrial tissue during vagal stimulation. *Proceedings of the 25th annual International Conference of the IEEE EMBS*, pages 167–170, 2003.
- [21] M. Courtemanche, R. J. Ramirez, and S. Nattel. Ionic mechanisms underlying human atrial action potential properties: insights from a mathematical model. *Am J Physiol*, 275(1):H301–21, 1998.
- [22] A. Tveito, G. T. Lines, M.M. Maleckar, and O. Skavhaug. Simplified mathematical models of defibrillation. *Conference Abstracts, Virtual Physiological Human Network of Excellence*, pages 367–369, 2010.
- [23] S. W. Morgan, G. Plank, I. V. Biktasheva, and V. N. Biktashev. Low energy defibrillation in human cardiac tissue: A simulation study. *Biophysical Journal*, 96:1364–1373, 2009.
- [24] A. Tveito and R. Winther. *Introduction to Partial Differential Equations*, volume 29 of *Texts in Applied Mathematics*. Springer, 1998.
- [25] Joakim Sundnes, Glenn Terje Lines, Xing Cai, Bjørn Fredrik Nielsen, Kent-Andre Mardal, and Aslak Tveito. *Computing the electrical activity in the heart*. Springer-Verlag, 2006.
- [26] Svein Linge, Joakim Sundnes, Monica Hanslien, Glenn Terje Lines, and Aslak Tveito. Numerical solution of the bidomain equations. *Philosophical Transactions of the Royal Society A*, 367(1895):1931–1951, 2009.
- [27] K.-A. Mardal, B.F. Nielsen, X. Cai, and A. Tveito. An order optimal solver for the discretized bidomain equations. *Numer. Linear Algebra Appl.*, 14:83–98, 2007.
- [28] J. Sundnes, R. Artebrant, O. Skavhaug, and A. Tveito. A second order algorithm for solving dynamic cell membrane equations. *IEEE Transactions on Biomedical Engineering*, 56(10):2546–2548, 2009.

<sup>1</sup>Simula Research Laboratory, Center for Biomedical Computing, P.O. Box 134, Lysaker 1325, Norway

<sup>2</sup>Department of Informatics, University of Oslo, P.O. Box 1072, 0316 Oslo, Norway